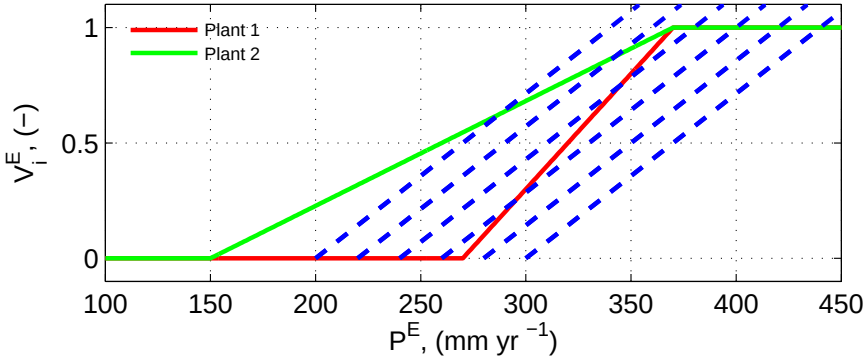

Figure 1. Vegetation–precipitation stability diagram (V_i^{E}, P^{E}) for two hypothetical plant types $i = 1, 2$ after Claussen et al., (2013). Full lines depict the equilibrium curves for vegetation cover $V_i^{\mathsf{E}}(P^{\mathsf{E}})$ for plant type 1 which is sensitive (red) and for plant type 2 which is resilient (green) to changes in precipitation. Dashed blue lines show hypothetical equilibrium precipitation curves $P^{\mathsf{E}}(V_i^{\mathsf{E}})$ for different time slices (4500, 4900, 5300, 5700, 6100, and 6500 years BP, from left to right). Intersections between the two types of curvesindicate equilibrium coupled states which can be stable or unstable.

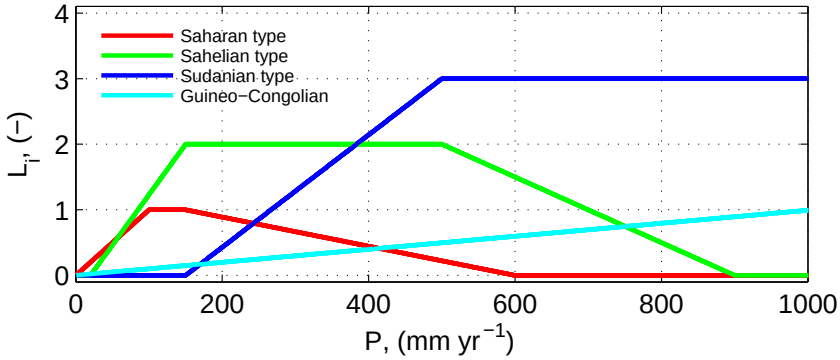

Figure 2. Environmental envelopes in terms of moisture requirements of four African Humid Period (AHP) plant types in the adjusted set up. The effective leaf area L_i is plotted as a function of mean annual precipitation P for the Saharan type (red), Sahelian type (green), Sudanian type (blue) and Guineo–Congolian type (light blue).

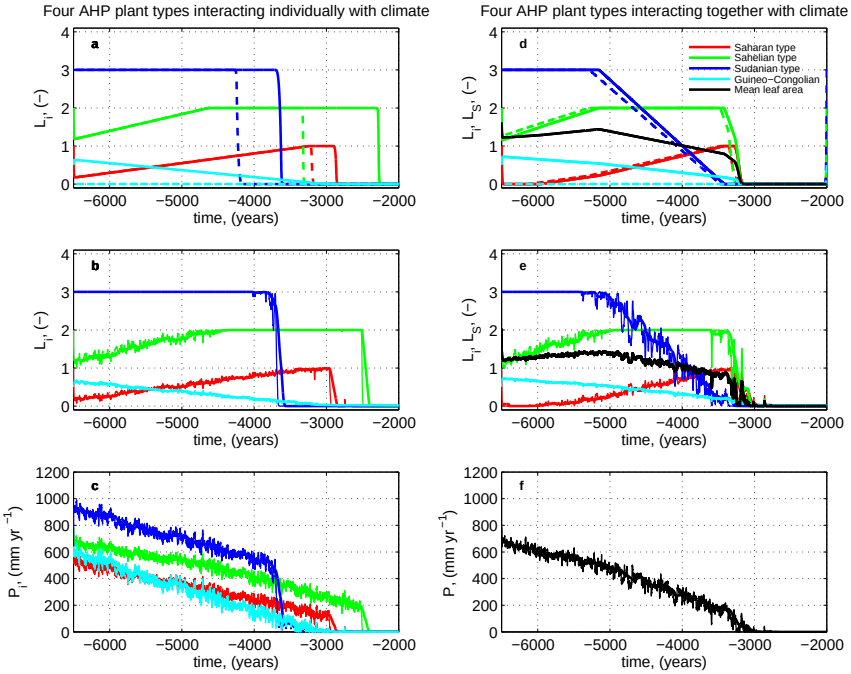

Figure 3. Transient dynamics of four African Humid Period (AHP) plant types interacting individually **(a–c)** and together **(d–f)** with climate. The effective leaf areas L_i and the corresponding precipitation amounts P_i are shown for the Saharan type (red), Sahelian type (green), Sudanian type (blue) and Guineo–Congolian type (light blue). Mean effective leaf area L_S and the corresponding precipitation P are calculated with the niche approach (black) (see Eq. 9). Simulations without background noise **(a, e)** include forward simulations (solid lines) and simulations backward in time (dashed lines). Simulations with background noise are depicted in **(b, e)** for L_i and L_S, and for precipitation P in **(c, f)**. Thin lines show annual mean values and thick lines show a 100 year running mean.

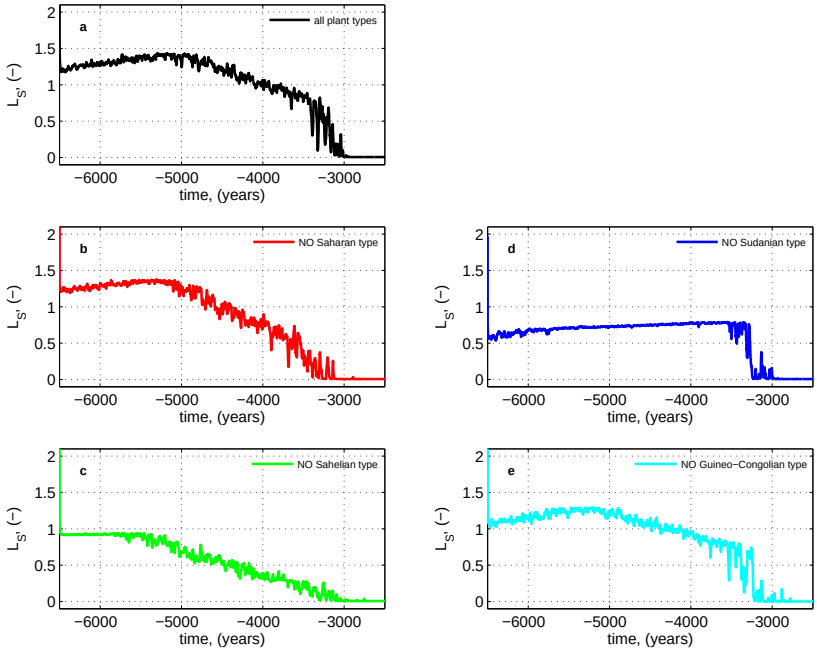

Figure 4. Transient dynamics of mean effective leaf area L_S illustrate the impact of the removal of plant types. Panels **(a–e)** show 100 year running means of different simulation set ups. The mean effective leaf area L_S accounting for all plant types ($N = n = 4$ in Eq. 10) is shown as a reference **(a)**. In each of the other simulations, one niche is not occupied ($N = 3$ and $n = 4$ in Eq. 10): no Saharan type **(b)**, no Sahelian type **(c)**, no Sudanian type **(d)** or no Guineo–Congolian type **(e)**.

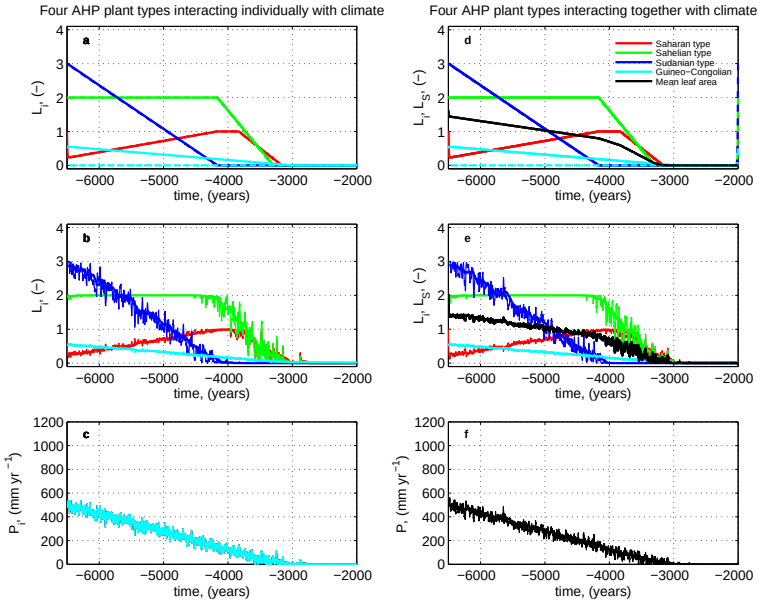

Figure 5. Transient dynamics of four African Humid Period (AHP) plant types interacting individually **(a–c)** and together **(d–f)** with climate for D_B = 0 mm yr^{-1}. The effective leaf areas L_i and the corresponding precipitation amounts P_i are shown for the Saharan type (red), Sahelian type (green), Sudanian type (blue) and Guineo–Congolian type (light blue). Mean effective leaf area L_S and the corresponding precipitation P are calculated with the niche approach (black) (see Eq. 9). Simulations without background noise **(a, e)** include forward simulations (solid lines) and simulations backward in time (dashed lines). Simulations with background noise are depicted in **(b, e)** for L_i and L_S, and for precipitation P in **(c, f)**. Thin lines show annual mean values and thick lines show a 100 year running mean.

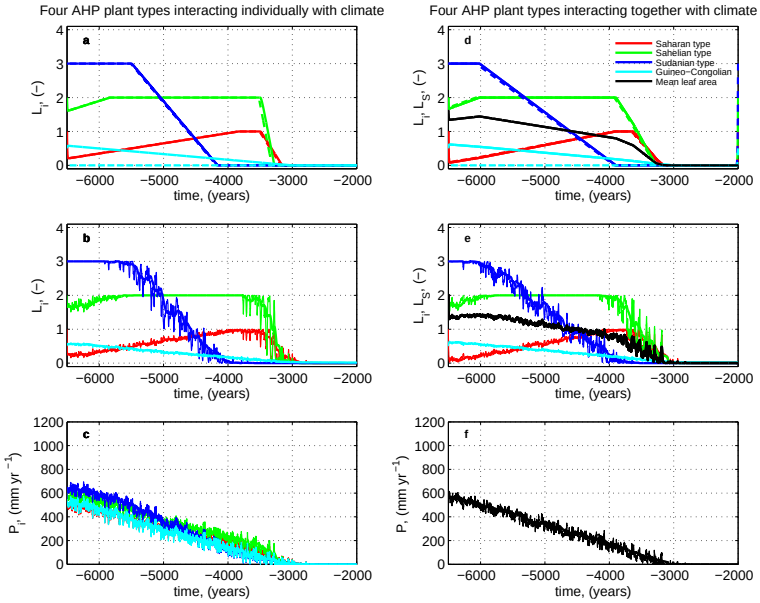

Figure 6. Transient dynamics of four African Humid Period (AHP) plant types interacting individually **(a–c)** and together **(d–f)** with climate for D_B = 50 mm yr^{-1}. The effective leaf areas L_i and the corresponding precipitation amounts P_i are shown for the Saharan type (red), Sahelian type (green), Sudanian type (blue) and Guineo–Congolian type (light blue). Mean effective leaf area L_S and the corresponding precipitation P are calculated with the niche approach (black) (see Eq. 9). Simulations without background noise **(a, e)** include forward simulations (solid lines) and simulations backward in time (dashed lines). Simulations with background noise are depicted in **(b, e)** for L_i and L_S, and for precipitation P in **(c, f)**. Thin lines show annual mean values and thick lines show a 100 year running mean.

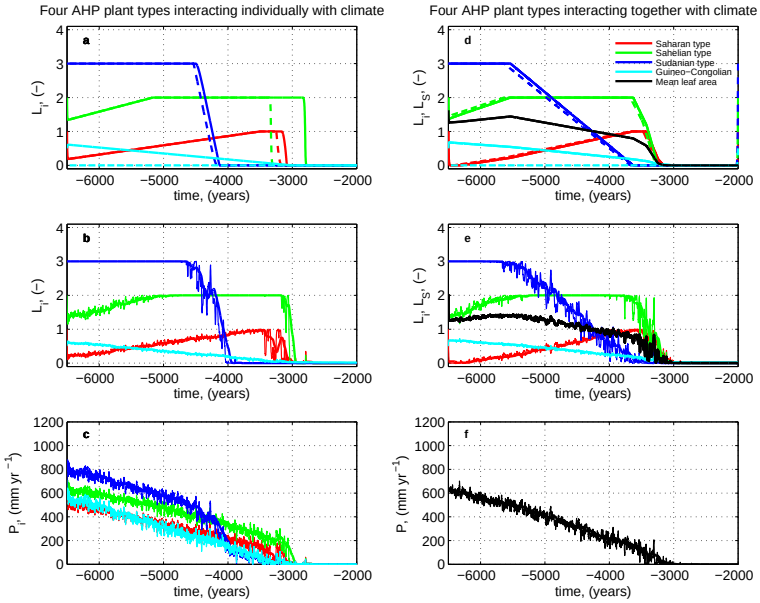

Figure 7. Transient dynamics of four African Humid Period (AHP) plant types interacting individually **(a–c)** and together **(d–f)** with climate for D_B = 100 mm yr^{-1}. The effective leaf areas L_i and the corresponding precipitation amounts P_i are shown for the Saharan type (red), Sahelian type (green), Sudanian type (blue) and Guineo–Congolian type (light blue). Mean effective leaf area L_S and the corresponding precipitation P are calculated with the niche approach (black) (see Eq. 9). Simulations without background noise **(a, e)** include forward simulations (solid lines) and simulations backward in time (dashed lines). Simulations with background noise are depicted in **(b, e)** for L_i and L_S, and for precipitation P in **(c, f)**. Thin lines show annual mean values and thick lines show a 100 year running mean.

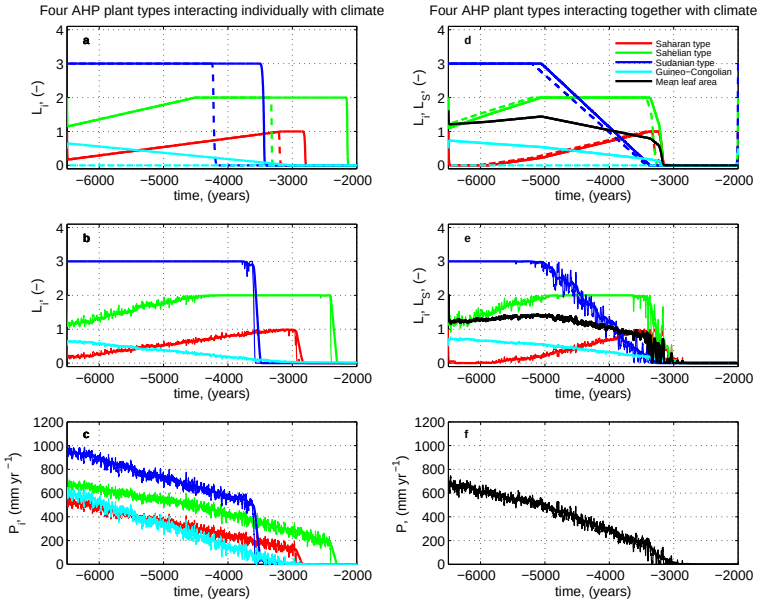

Figure 8. Transient dynamics of four African Humid Period (AHP) plant types interacting individually **(a–c)** and together **(d–f)** with climate for D_B = 150 mm yr^{-1}. The effective leaf areas L_i and the corresponding precipitation amounts P_i are shown for the Saharan type (red), Sahelian type (green), Sudanian type (blue) and Guineo–Congolian type (light blue). Mean effective leaf area L_S and the corresponding precipitation P are calculated with the niche approach (black) (see Eq. 9). Simulations without background noise **(a, e)** include forward simulations (solid lines) and simulations backward in time (dashed lines). Simulations with background noise are depicted in **(b, e)** for L_i and L_S, and for precipitation P in **(c, f)**. Thin lines show annual mean values and thick lines show a 100 year running mean.

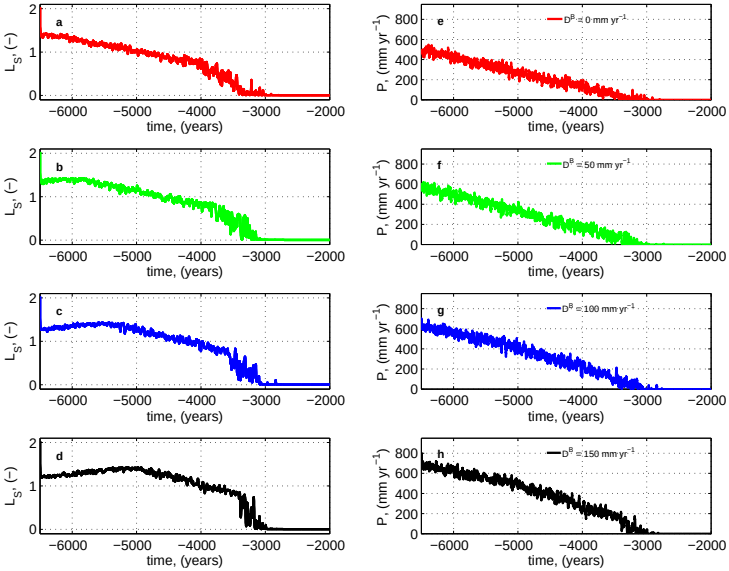

Figure 9. Transient dynamics of mean effective leaf area L_S of four African Humid Period (AHP) plant types interacting together with climate, and the corresponding precipitation P for different feedback sensitivity coefficients D^B. Simulations with background noise are depicted in **(a–d)** for L_S, and for mean annual precipitation P in **(e–h)** for D^B = 0 mm yr^{-1} (red), D^B = 50 mm yr^{-1} (green), D^B = 100 mm yr^{-1} (blue), and D^B = 150 mm yr^{-1}(black). Without feedback between vegetation and precipitation **(a, e)**, L_S and corresponding P decrease almost linearly. Low feedback coefficients **(b, f)** result in a non-linear but gradual decline of L_S and corresponding P with small fluctuations. The higher D_B, the stronger the amplitude of fluctuations and the steeper the decline of L_S and corresponding P.

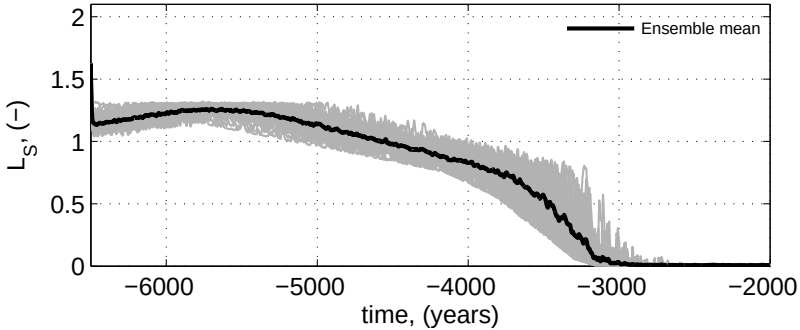

Figure 10. Mean effective leaf area L_S of four African Humid Period (AHP) plant types *i* interacting together with climate with different sets of specific climate feedback coefficients D_i^B. 30 simulations with different variations of D_i^B in the range from 0 to 150 $\mathrm{mm\,yr}^{-1}$ are shown in gray, the ensemble mean is shown in black.